CATENA-01240; No of Pages 10

Available online at www.sciencedirect.com
ScienceDirect

Catena xx (2007) xxx–xxx

CATENA

www.elsevier.com/locate/catena

Sand detachment under rains with varying angle of incidence

G. Erpul [a,*], D. Gabriels [b], W.M. Cornelis [b], H.N. Samray [a], T. Guzelordu [a]

[a] Department of Soil Science, Faculty of Agriculture, University of Ankara, 06110 Diskapi-Ankara, Turkey
[b] Department of Soil Management and Soil Care, Ghent University, Coupure Links 653, B 9000 Ghent, Belgium

Received 5 April 2007; received in revised form 11 July 2007; accepted 21 July 2007

Abstract

In the case of wind-driven rain, as the angle of rain incidence increases, greater force components act parallel to the surface and lower force components act perpendicular to the surface. Therefore, raindrop impact angle could influence the detachment process in the existence of substantial lateral jet development. This could be particularly significant for a cohesionless sand surface that has a weaker resistance to the dislodgement by a raindrop impact than a soil surface. Experiments of simulated wind-driven rain were conducted to evaluate sand detachment rates under increased lateral jetting induced by wind velocities of 6.4, 10.0, and 12.0 m s^{-1} at nozzle operating pressures of 75, 100, and 150 kPa and incident on windward and leeward slopes of 4 and 9°. With these set-ups, it was possible to have varying angles of incidence and to determine the effect of the compressive stress and shear stress, evaluated by the horizontal and vertical kinetic energy fluxes (E_{tx} and E_{tz}, respectively), on the detachment rates from the sand surface. At the same vectorwise sum of E_{tz} and E_{tx}, the results showed that there was, for similar values of E_{tz} and E_{tx} in windward slopes, more sand detachment rate; however, for dissimilar values of E_{tz} and E_{tx} in leeward slopes where E_{tx} was significantly higher than E_{tz}, there was less sand detachment rate. Consequently, with certain values of the compressive stress and shear stress, the sand detachment rates under wind-driven rains peaked; and E_{tz} was the limiting component since the rates significantly decreased as E_{tz} particularly decreased in spite of very large values of E_{tx}.

Keywords: Sand detachment; Angle of rain incidence, Compressive stress; Shear stress

1. Introduction

Mostly by laboratory experiments, the process of soil detachment as a result of raindrop impact was studied by many researchers (Ellison, 1947; Young and Wiersma, 1973; Morgan, 1978; Poesen and Savat, 1981; Ghadiri and Payne, 1981, 1986, 1988; Poesen and Torri, 1988; Sharma and Gupta, 1989; Salles and Poesen, 2000; Ghadiri, 2004). In these studies, a spherical raindrop vertically striking a soil or sand surface was used to explain the process (Sharma et al., 1991, 1995). Physical raindrop characteristics such as size, speed, and frequency were commonly linked with the process of detaching soil particles by raindrop impact (Meyer, 1981; Kinnell, 1981; Park et al., 1983; Hairsine and Rose, 1991; Erpul et al., 2005). When raindrops impact a loose sediment surface, they transfer part of their momentum to the particles, and with this particles are launched into arched trajectories away from raindrop impact sites (Savat and Poesen, 1981; Poesen, 1985; Erpul et al., 2003; Cornelis et al., 2004b,c; Furbish et al., 2007).

During a raindrop impact, the pressure builds up at the raindrop–soil interface and the high pressure inside the raindrop then forces the water to escape laterally (Springer, 1976). Basically, as falling raindrops hit the surface, soil particles broken away from the aggregates splash into the air and soil detachment takes place. More distinctively, two forms of movement of the splash phenomenon were explained by Huang et al. (1982): the compressive stress from the impact and the shear stress from the lateral jetting were those that caused the phenomenon. In their numerical simulations with a spherical raindrop hitting a rigid surface perpendicularly, they concluded that the maximum pressure occurred at the circumference of the raindrop contact surface. Accordingly, Al-Durrah and Bradford (1982) particularized the phenomenon how compressive stress was transformed to or compensated by lateral shear stress resulting from radial flow of the striking drop. Later, Huang et al. (1983) reported that, when

* Corresponding author. Tel.: +90 312 596 1796; fax: +90 312 317 8465.
E-mail address: erpul@agri.ankara.edu.tr (G. Erpul).

0341-8162/$ - see front matter © 2007 Elsevier B.V. All rights reserved.
doi:10.1016/j.catena.2007.07.008

Please cite this article as: Erpul, G. et al. Sand detachment under rains with varying angle of incidence. Catena (2007), doi:10.1016/j.catena.2007.07.008

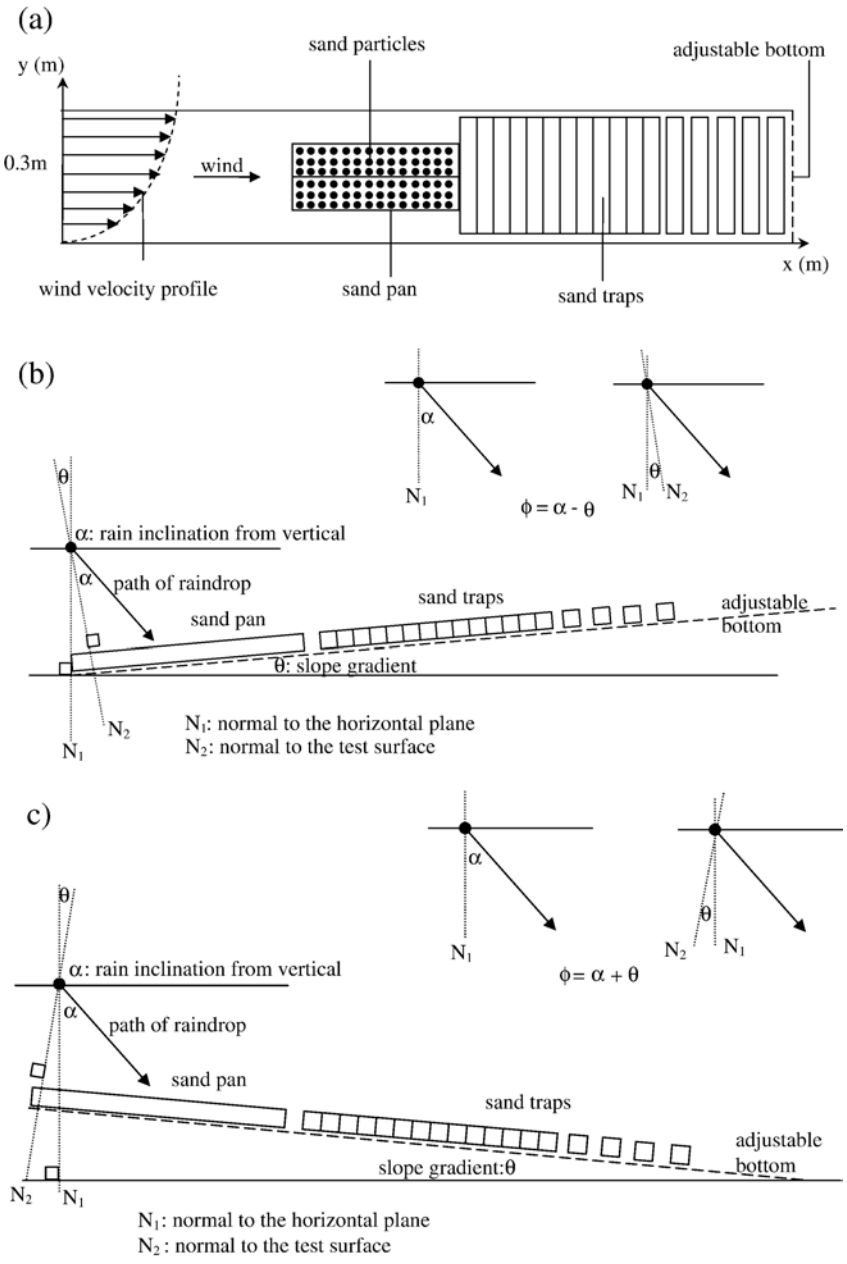

Fig. 1. Experimental set-up with sand pan and traps for measurement of sand detachment (a) plan view, (b) side view of windward set-up, and (c) side view of leeward set-up (Note that the figure is not to scale).

a raindrop impacts on rigid surfaces, the lateral jet development would be greater than that when it hits a soft and elastic surface. These results show that the partition of the compressive and tangential forces could significantly determine the magnitude of the soil detachment process, which on a cohesionless surface could differ from that on a cohesive one.

It is clear that the incidence angle of raindrop impact differs considerably from the vertical under which most of the controlled studies were conducted. In terms of the influence of the stress partition on the detachment process, the relative contribution of the compressive and tangential forces in a vertically striking raindrop is likely to be different from that of the drop hitting on a surface with a given degree of angle; that is, compressive stress of the impact decreases as rain inclination from the vertical increases and the shear stress accordingly becomes stronger. Also, apart from being the radial, splashes tend to be unidirectional in the favor of prevailing action of wind (De Lima, 1989) or slope (Poesen, 1985; Erpul et al., 2005). Cruse et al. (2000) and Erpul (2001) reported that the angle of incidence of raindrop impact varies significantly and would greatly depend on wind speed and slope aspect of topography during most rainfall.

There are only few studies on the effect of impact angle on soil detachment. Regardless of the stress partition, Van Heerden (1964) observed that soil detachment decreased under wind-driven rains. The same results were found by Erpul et al. (2003)

Please cite this article as: Erpul, G. et al. Sand detachment under rains with varying angle of incidence. Catena (2007), doi:10.1016/j.catena.2007.07.008

in the study of the effect of wind on the raindrop impact and soil detachment. Subsequently, Erpul et al. (2005) showed that the vertical compressive stress of a wind-driven raindrop impact grew weaker as the raindrop deviated from the vertical and the tangential shear stress went stronger and controlled the sand detachment rates from the splash cups, and the sand detachment increased with the angle of incidence consequent to the horizontal wind speed. These sand detachment results on sand (Erpul et al., 2005) disagreed with those observed for soil (Erpul et al., 2003); regarding detachment under the rains with varying angle of incidence the sand surfaces behaved different from the soil surfaces. Also, these studies clearly indicated that the relative contribution of the vertical and horizontal components of impact stress varied in detachment and this could likely depend on the strength of the raindrop-impacted surface. Although "soil" is used as a more general term that also includes "sand", in the process of soil detachment by the raindrop impact, Erpul (2003) and Erpul et al. (2005) distinguished both in terms of cohesion since cohesive soils are generally characterized by smaller particle sizes than cohesionless sand. Cruse et al. (2000) showed that there were significant soil detachment interactions resulting from different mechanical behavior of the soil surfaces and the lateral jets of varying impact angles. Their fairly divergent results of soil detachment accounted for the differences in elasticity of waterdrop–soil collision and influence of drop impact angle on lateral jets. For example, with the weak loess soil and perpendicular raindrop impacts, lateral jet development, other than shear strength, restricted measured detachment, and it appeared that soil detachment increased at lower impact angles since lateral jets were more efficient in detaching particles from the point of impact. Depending on elasticity or rigidity of the surface (Huang et al., 1982, 1983), soil detachment varied with the development of lateral jets (Cruse et al., 2000). Huang et al. (1983) reported that the lateral jet of water from raindrop impact would be greater on rigid surfaces and for lower impact angles than that on a soft, elastic surface with raindrop impact at a perpendicular angle. Obviously, in the situations where the increased lateral jetting by wind drive exists, as the raindrop impact angle decreases (Cruse et al., 2000; Erpul, 2001), greater force components act parallel to the surface and lower force components act perpendicular to the surface.

Table 1
Calculated correction factors using rain inclination, slope gradient, and slope aspect

u (m s^{-1})	α (°)	θ (°)	η_{ww} (1+tan α tan θ)	η_{lw} (1−tan α tan θ)
6.4	55	4	1.10	0.90
		9	1.23	0.77
10.0	68	4	1.17	0.83
		9	1.40	0.60
12.0	72	4	1.22	0.78
		9	1.49	0.51

u: reference horizontal wind velocity; α: rain inclination from vertical (the angle of rain inclination was approximately 55, 68, and 72° for the wind-driven rain with 6.4, 10.0, and 12 ms^{-1}, respectively (Erpul et al., 2005); θ: slope gradient; η_{ww}: correction factor for windward slopes; η_{lw}: correction factor for leeward slopes.

Table 2
Rain intensities measured in the horizontal plane for nozzle operating pressures of 75, 100, and 150 kPa and wind velocities of 6.4, 10.0, and 12 ms^{-1}

u (m s^{-1})	P (kPa)	I_h* (mm h^{-1})
6.4	75	113±18
	100	116±10
	150	124±10
10.0	75	108±21
	100	110±10
	150	136±19
12.0	75	110±20
	100	115±19
	150	139±13

*Subscript "h" signs that intensity was measured in the horizontal plane.

This study examines sand detachment under wind-induced lateral jetting and investigates the relative effects of the different components the raindrop incidence vector on sand detachment. The relative importance of the two stress components in soil detachment has not yet been explicitly explored, and therefore, the precision of components in detachment quantification will be useful. The role of horizontal and vertical energy components of raindrops hitting the sand surface with varying angle of incidence in sand detachment is presented in this article.

2. Material and methods

Experiments were conducted under laboratory conditions in the wind tunnel rainfall simulator facility of the International Center for Eremology, Ghent University, Belgium (Gabriels et al., 1997; Cornelis et al., 2004a). The test section of the tunnel is 1·20 m wide and 12 m long and has a ceiling adjustable in height from 1·80 m to 3·20 m. Wind velocity profiles were measured from the sand surface up to 2-m nozzle height with a vane anemometer and associated recording equipment. The boundary layer in the test section was set at a 0.30 m thickness above the sand pan, and subsequently the reference wind velocities were derived from the logarithmic wind profiles assuming a fixed roughness height 0.0001 m for the smoothed sand surface (Fig. 1a) (Erpul, 2001).

The rainfall simulator consisted of a pipeline with spray nozzles. In this study, we used a continuous spraying system of ten downward-oriented nozzles installed 2 m high and at 1 m intervals over a length of 12 m. Three operating nozzle pressures were applied, which were 75, 100, and 150 kPa. Tap water was used with an electrical conductivity at 25 °C of 0.7 dS m^{-1}. Cumulative volume percentage of the raindrop size distributions for the simulated wind-driven rains at different operating pressures are given by Cornelis et al. (2004a) by the logistic growth models ($R^2 \geq 0.99$). The median raindrop diameters obtained under both different operating pressures and different wind speeds varied from 1.53 to 1.63 mm (Erpul, 1996; Erpul et al., 1998; Cornelis et al., 2004a).

The material used in this study of wind-driven rain was very well sorted dune sand collected from the Belgian coast. The particle-size ranges that were used consisted of 100–200, 200–500, and 50–500 μm for the dune sand, of which geometric particle diameter was 250 μm. Its calcium carbonate and

Please cite this article as: Erpul, G. et al. Sand detachment under rains with varying angle of incidence. Catena (2007), doi:10.1016/j.catena.2007.07.008

Table 3
Calculated number of raindrops (n, # m^{-2} s^{-1}) from I_c* (mm h^{-1}) and calculated angle of rain incidence as a function of the rain inclination, slope gradient and aspect together with its horizontal and vertical components for the rains driven by the reference wind velocities of 6.4, 10.0, and 12.0 m s^{-1}

u (ms^{-1})	α (°)	θ (°)	P (kPa)	d_{50} (mm)	Windward					Leeward				
					I_c (mm h^{-1})	n (# m^{-2} s^{-1})	$\phi=\alpha-\theta$ (°)	sin ϕ	cos ϕ	I_c (mm h^{-1})	n (# m^{-2} s^{-1})	$\phi=\alpha+\theta$ (°)	sin ϕ	cos ϕ
6.4	55	4.0	75	1.62	125	1.54E+04	51	0.7771	0.6293	102	1.28E+04	59	0.8572	0.5150
			100	1.58	128	1.71E+04				105	1.42E+04			
			150	1.63	136	1.66E+04				112	1.38E+04			
		9.0	75	1.64	139	1.71E+04	46	0.7193	0.6947	87	1.11E+04	64	0.8988	0.4384
			100	1.67	143	1.90E+04				90	1.23E+04			
			150	1.52	152	1.84E+04				96	1.20E+04			
10.0	68	4.0	75	1.61	127	1.53E+04	64	0.8988	0.4384	89	1.07E+04	72	0.9511	0.3090
			100	1.53	130	1.48E+04				92	1.04E+04			
			150	1.55	160	2.42E+04				113	1.70E+04			
		9.0	75	1.62	151	1.82E+04	59	0.8572	0.5150	65	7.79E+03	77	0.9744	0.2250
			100	1.58	155	1.77E+04				67	7.58E+03			
			150	1.63	191	2.89E+04				83	1.24E+04			
12.0	72	4.0	75	1.64	134	1.72E+04	68	0.9272	0.3746	86	1.08E+04	76	0.9703	0.2419
			100	1.67	140	2.10E+04				91	1.32E+04			
			150	1.52	169	2.43E+04				109	1.53E+04			
		9.0	75	1.61	164	2.13E+04	63	0.8910	0.4540	56	6.67E+03	81	0.9877	0.1564
			100	1.53	172	2.60E+04				59	8.15E+03			
			150	1.55	208	3.02E+04				71	9.45E+03			

u = Horizontal wind velocity; α = rain inclination from vertical; θ = slope gradient; d_{50} = median drop size; ϕ = angle of rainfall incidence; ww: windward, lw: leeward.
*I_c is calculated by $I_c=\eta I_h$ using wind-driven intensity measured in the horizontal plane (I_h, mm h^{-1}) and the correction factor (η), and subscript "c" signs that intensity was calculated from that measured in the horizontal plane.

organic matter content were 3.34% and 0%, respectively. The electrical conductivity of the sand was 0.72 dS m^{-1} at 25 °C and the bulk density was 1.7 Mg m^{-3} (Cornelis et al., 2004b,c). The sand was placed into a 55-cm long and 20-cm wide pan which was located at a distance x=6.45 m downwind from the entrance of the wind tunnel working section along its centerline (Fig. 1a). The sand pan had a perforated bottom to allow free drainage. Each run was performed on a pre-wetted sand surface to prevent sand from lifting off due to the wind. The surface was pre-wetted by spraying it with tap water before it was exposed to the wind-driven rain and was smoothed exactly on a level with the rim of the pan. Accordingly, there was only raindrop-induced, no wind-induced, particle entrainment in the experiment Cornelis et al., 2004b,c).

The rains driven by horizontal wind velocities 6.4, 10.0, and 12.0 ms^{-1} were applied to the sand pan placed at both windward and leeward slopes of 7% and 16% (4.0° and 9.0°, respectively). For each slope aspect there were two replicates

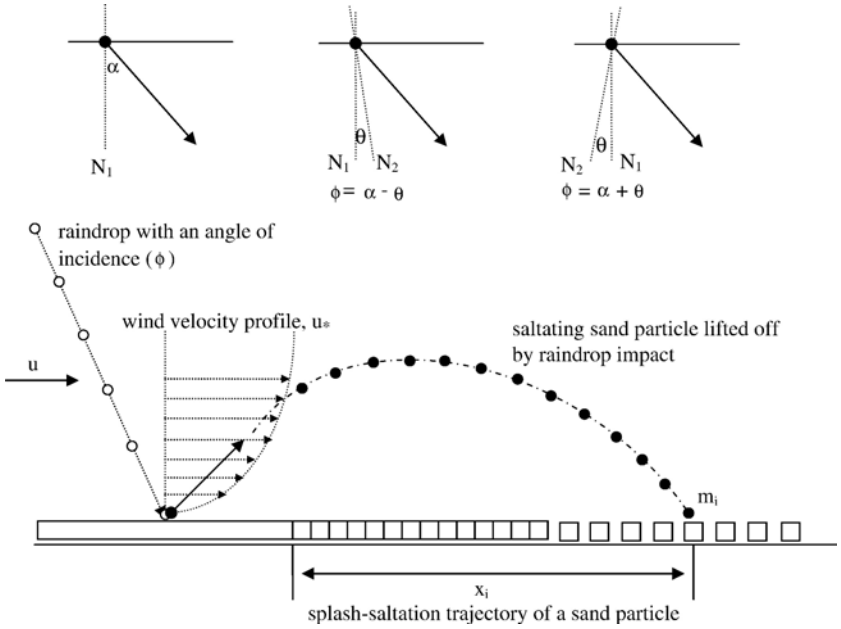

Fig. 2. Rainsplash transport: raindrop-induced and wind-driven splash trajectories of sand particles falling through a wind profile.

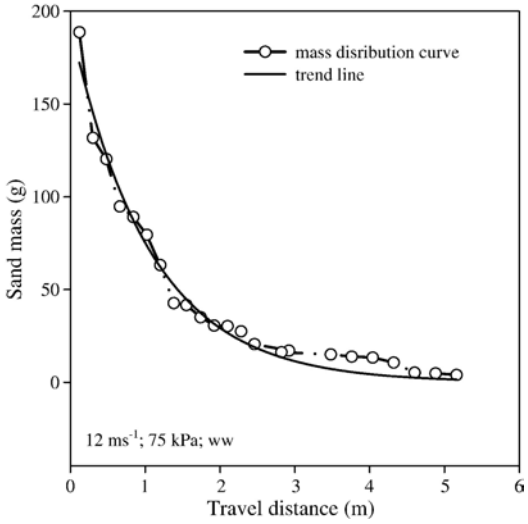

Fig. 3. Exponential decay curve of sand mass (m_i) versus travel distance (x_i) used for calculating the sand detachment rate by Eqs. (10) and (11).

(36 runs), and with 3 nozzle pressures × 3 wind velocities × 2 slope gradients × 2 replicates, and thus a total of 72 rainfall simulations were conducted (Fig. 1b and c).

The spatial distribution of the wind-driven rain intensity on a horizontal plane in the tunnel was obtained on a horizontal plane by mapping the pattern of iso-lines and locating the most available working area in the tunnel (Erpul et al., 1998). The uniformity coefficients of the rainfall intensity changed from 82% for the rains driven by wind speed of 12.0 ms^{-1} with the nozzle pressure of 75 kPa to 92% for those driven by 6.4 ms^{-1} with the nozzle pressure of 150 kPa (Erpul, 1996). The actual amount of rain intercepted on a sloping surface with respect to the prevailing wind direction was calculated with the angle of rain incidence using the correction factors (Sharon, 1970, 1980; Sharon et al., 1983, 1988; De Lima, 1990; Sharon and Arazi, 1997; Blocken and Carmeliet, 2000, 2002, 2004; Blocken et al., 2005; Cornelis et al., 2004a; Blocken et al., 2006):

$$\eta = 1 \pm \tan\alpha \tan\theta \cos(z_\alpha \pm z_\theta) \quad (1)$$

where, η is a correction factor that in fact indicates catch ratio when wind-driven rain is intercepted by sloping surface compared to that by the horizontal plane, α is the raindrop inclination from vertical; θ is the slope gradient; and z_α and z_θ are the azimuth from which rain is falling and azimuth towards which the plane of surface is inclined, respectively. The positive sign shows windward facing slope and the negative sign corresponds to leeward facing slope, implying raindrop deficit with the same values of α and θ. In our experimental set-up, the wind direction from which rain fell and the plane of surface on which the sand pan were placed were on the same axis, therefore, since $z_\alpha = 0$, $z_\theta = 0$, and $\cos(z_\alpha \pm z_\theta) = 1$, Eq. (1) reduced to Eq. (2):

$$\eta = 1 \pm \tan\alpha \tan\theta \quad (2)$$

The mean angle of rain inclination from the vertical was calculated analytically using the direct intensity measurements in the tunnel (Erpul et al., 2005). The variation of α (°) with respect to horizontal reference wind speed (u, ms^{-1}) is given by Eq. (3) (Erpul et al., 2005):

$$\frac{\partial(\alpha)}{\partial u} = 0.0429u^2 - 1.455u + 12.685 \quad (3)$$

Calculated correction factors by Eq. (2) are given in Table 1 for rain inclinations of 55, 68, and 72° resulting from the horizontal wind velocities of 6.4, 10.0, and 12.0 ms^{-1} and the gradients of 4 and 9° of the windward and leeward slopes. Rain intensities measured in the horizontal plane (I_h, mm h^{-1}) for nozzle operating pressures of 75, 100, and 150 kPa at the given wind velocities are given in Table 2, and calculated wind-driven intensities (I_c, mm h^{-1}) for windward and leeward slopes of 4 and 9° are tabulated in Table 3.

The resultant velocity (V_r, ms^{-1}) and energy (E_r, J) of simulated rainfalls were measured by a Sensit kinetic energy sensor (Sensit, 2000) and variations of both with respect to u were given respectively by (Erpul et al., 2003):

$$\frac{\partial(V_r)}{\partial u} = 0.26e^{0.10u} \quad (4)$$

$$\frac{\partial(E_r)}{\partial u} = 1.47 \times 10^{-6} e^{0.18u} \quad (5)$$

The total resultant kinetic energy flux of raindrops (E_t, J m^{-2} s^{-1}) was calculated considering the representative raindrop sizes (d_{50}) as functions of both horizontal wind speed and nozzle operating pressure (Erpul et al., 1998, 2000):

$$E_t = \left[k \sum_{i=1}^{n} d_i^3 V_{ri}^2 n_i \right] A^{-1} t^{-1} \quad (6)$$

where, n_i is the number of raindrop diameter classes, d_i is the mean diameter for diameter class i (m), V_{ri} is the resultant impact velocity of raindrop diameter d_i (m s^{-1}), k is the product of all constants of the equation, and A and t are the sampling area and time over which the sample is taken, respectively. Eq. (6) is in fact the resultant kinetic energy (E_r, J) multiplied by the

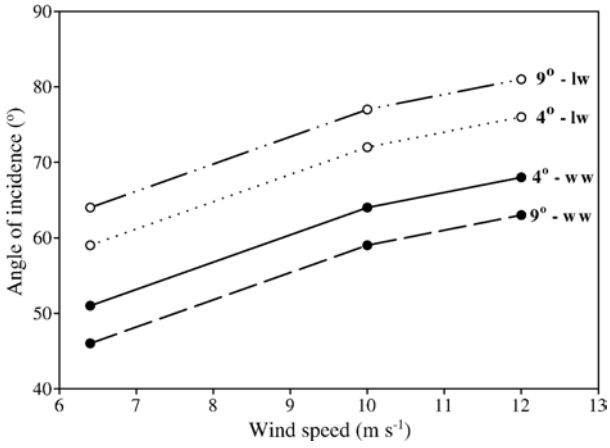

Fig. 4. Angle of rain incidences for the rains driven by the reference wind speeds of 6.4, 10.0, and 12.0 m s^{-1}.

Please cite this article as: Erpul, G. et al. Sand detachment under rains with varying angle of incidence. Catena (2007), doi:10.1016/j.catena.2007.07.008

total number of raindrops per unit area per unit time, which was estimated using the calculated wind-driven intensities (I_c, m s^{-1}) for windward and leeward slopes of 4 and 9° (Table 3) by Eq. (7):

$$n_i = \frac{I_c A t}{\forall_i} \tag{7}$$

where, $A=\pi(d_{50})^2/4$ (m^2), $\forall=\pi(d_{50})^3/6$ (m^3), and t is time of sampling (s). In this study, median raindrop diameters (d_{50}) were used in Eqs. (6) and (7) as a representative characteristic of the wind-driven rain size distributions. The horizontal and vertical kinetic energy fluxes (E_{tx} and E_{tz} in J m^{-2} s^{-1}, respectively) were computed using the angle of rain incidences (ϕ) (Fig. 1b and c) by:

$$E_{tx} = E_t \sin^2\phi \tag{8}$$

$$E_{tz} = E_t \cos^2\phi \tag{9}$$

Eqs. (8) and (9) integrate the effect of wind on raindrop impact velocity, impact frequency, and impact angle.

Sand detachment rates were evaluated by the amount of splashed particles trapped at set distances on a 7-m uniform slope segment. Troughs (1.20 m × 0.14 m = 0.168 m^2) were placed in the upslope and downslope direction, respectively, for the windward and leeward slopes (Fig. 2). The sand particles trapped in the collecting troughs were washed, oven-dried, and weighed. Exponential decay curves of the trapped sand amount (g) vs. the splash distance (m) (Eq. (10)) were used to approximate the sand detachment rates (Savat and Poesen, 1981; Poesen, 1985; Erpul et al., 2004; Furbish et al., 2007) (Fig. 3) by Eq. (11) (Erpul et al., 2003):

$$m_i = \beta e^{-\delta x_i} \tag{10}$$

where, m_i is the mass of soil splashed over the distance x_i, and β and δ are coefficients that depend upon the physical properties of sand particles. Respectively for windward and leeward slopes, coefficient values were $746 \le \beta \le 2290$ and $31 \le \beta \le 254$, and $1.50 \le \delta \le 3.98$ and $0.80 \le \delta \le 3.83$. The detachment rate was then calculated as:

$$D = \frac{1}{At}\int \frac{m_i}{x_i}\partial x \tag{11}$$

where, D is the sand detachment rate (g m^{-2} min^{-1}), A is the surface area of sand pan (0.55 m × 0.20 m = 0.110 m^2), and t is the time of sampling (45 min).

3. Results and discussion

The characteristics of the wind-driven rains such as the calculated the number of raindrops and angle of rain incidences as a function of the rain inclination and slope gradient and aspect together with its horizontal and vertical components for the rains driven by the reference wind velocities of 6.4, 10.0, and 12.0 m s^{-1} are given in Table 3.

The range of angle of incidences (ϕ) and their vertical and horizontal components (cos ϕ and sin ϕ, respectively) can be observed from Fig. 4 and Table 3, respectively. The bounds of

Table 4
Summary of the data of kinetic energy fluxes and measured detachment rates for the rains driven by the reference wind velocities of 6.4, 10.0, and 12.0 m s^{-1}

u (ms^{-1})	α (°)	θ (°)	P (kPa)	Windward						Leeward					
				E_t (J $m^{-2}s^{-1}$)	E_{tz} (J $m^{-2}s^{-1}$)	E_{tx} (J $m^{-2}s^{-1}$)	E_{tx}/E_{tz}	D (g m^{-2} min^{-1})		E_t (J $m^{-2}s^{-1}$)	E_{tz} (J $m^{-2}s^{-1}$)	E_{tx} (J $m^{-2}s^{-1}$)	E_{tx}/E_{tz}	D (g m^{-2} min^{-1})	
								Mean	SD					Mean	SD
6.4	55	4.0	75	0.344	0.148	0.196	1.32	28.63	0.94	0.285	0.085	0.201	2.36	4.90	0.06
			100	0.381	0.164	0.217	1.32	43.74	0.41	0.316	0.094	0.222	2.36	6.34	0.76
			150	0.369	0.159	0.210	1.32	45.49	11.91	0.307	0.091	0.216	2.37	5.29	0.48
		9.0	75	0.381	0.198	0.183	0.92	40.06	0.69	0.248	0.054	0.193	3.57	3.84	0.44
			100	0.422	0.219	0.203	0.93	54.58	6.04	0.274	0.060	0.214	3.57	6.91	1.36
			150	0.410	0.213	0.197	0.92	44.49	3.10	0.266	0.058	0.208	3.59	4.75	1.66
10.0	68	4.0	75	0.813	0.154	0.659	4.28	128.76	0.13	0.571	0.053	0.518	9.77	13.25	2.87
			100	0.791	0.150	0.641	4.27	129.79	4.79	0.555	0.052	0.504	9.69	9.65	1.05
			150	1.292	0.245	1.047	4.27	144.45	10.48	0.907	0.085	0.823	9.68	25.63	4.24
		9.0	75	0.969	0.255	0.714	2.80	148.51	0.02	0.415	0.020	0.395	19.75	5.44	1.84
			100	0.942	0.248	0.694	2.80	142.45	0.96	0.404	0.020	0.384	19.20	6.96	1.00
			150	1.540	0.406	1.134	2.79	138.93	5.35	0.660	0.032	0.628	19.63	12.53	3.04
12.0	72	4.0	75	1.417	0.174	1.243	7.14	151.78	3.61	0.890	0.042	0.848	20.19	23.07	0.44
			100	1.732	0.212	1.520	7.17	172.89	6.40	1.087	0.051	1.036	20.31	26.24	2.69
			150	2.008	0.246	1.762	7.16	187.71	4.73	1.261	0.059	1.202	20.37	28.45	1.94
		9.0	75	1.757	0.328	1.429	4.36	172.93	3.76	0.550	0.009	0.541	60.11	7.45	1.14
			100	2.148	0.401	1.747	4.36	203.44	0.43	0.672	0.011	0.661	60.09	13.69	2.21
			150	2.490	0.465	2.025	4.35	207.16	2.94	0.779	0.013	0.766	58.92	21.96	0.32

u = Horizontal wind velocity; α = rain inclination from vertical; θ = slope gradient; E_t = resultant energy flux; E_{tz} = energy flux calculated using vertical component of impact velocity; E_{tx} = energy flux calculated using horizontal component of impact velocity; D = sand detachment rate; SD = standard deviation for detachment rate.

Please cite this article as: Erpul, G. et al. Sand detachment under rains with varying angle of incidence. Catena (2007), doi:10.1016/j.catena.2007.07.008

ϕ, cos ϕ, and sin ϕ were $51 \le \phi \le 81$, $0.16 \le \cos\phi \le 0.69$, and $0.78 \le \sin\phi \le 0.99$, respectively. These showed that, since the compressive and shear stresses of the wind-driven raindrops varied respectively with cos ϕ and sin ϕ, proportionally the former attained to a value as low as 0.16 and the latter to as a high value as 0.99. Since both act inversely, they occurred in the rain driven by a 12.0 ms^{-1} wind incident on the leeward slope of 9°. For the most part, the study was performed with the increased lateral jets of the wind-driven raindrops (Table 3 and Fig. 4).

Total resultant kinetic energy fluxes computed using the resultant raindrop impact velocity and the number of wind-driven raindrops by Eq. (6) as functions of both horizontal wind velocities (6.4, 10.0, and 12.0 m s^{-1}) and nozzle operating pressures (75, 100, and 150 kPa) are tabulated in Table 4 and graphed in Fig. 5.

Graphs revealed that total kinetic energy flux (E_t, J m^{-2} s^{-1}) increased as wind speed (u, m s^{-1}) increased at each level of the nozzle operating pressure (P, kPa), and for a particular wind speed E_t was greater in the windward slopes than in the leeward slopes. This was because the leeward slopes received less raindrop impact than the windward slopes (Table 3).

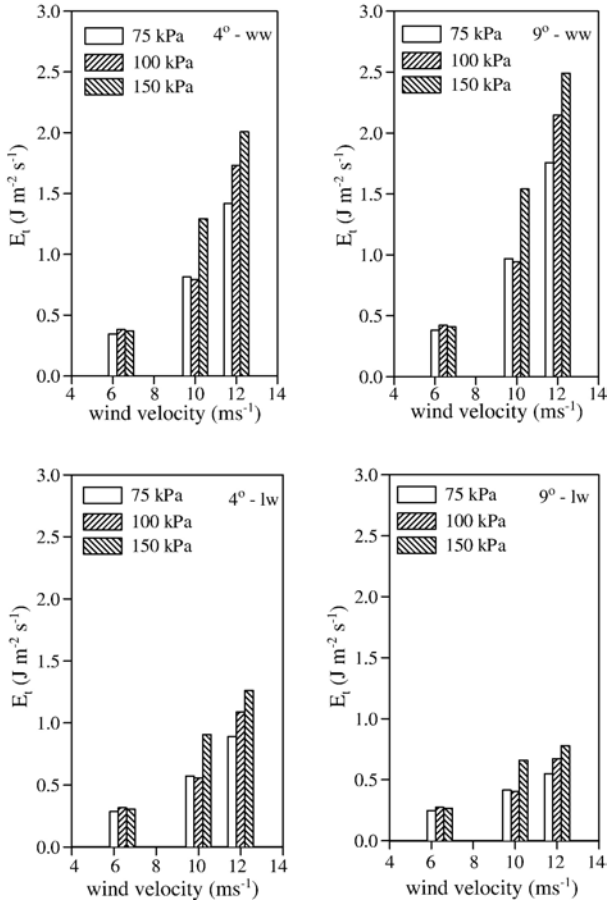

Fig. 5. Total resultant kinetic energy fluxes computed using the resultant raindrop impact velocity and the number of wind-driven raindrops by Eq. (6) as functions of both horizontal wind velocity and nozzle operating pressure.

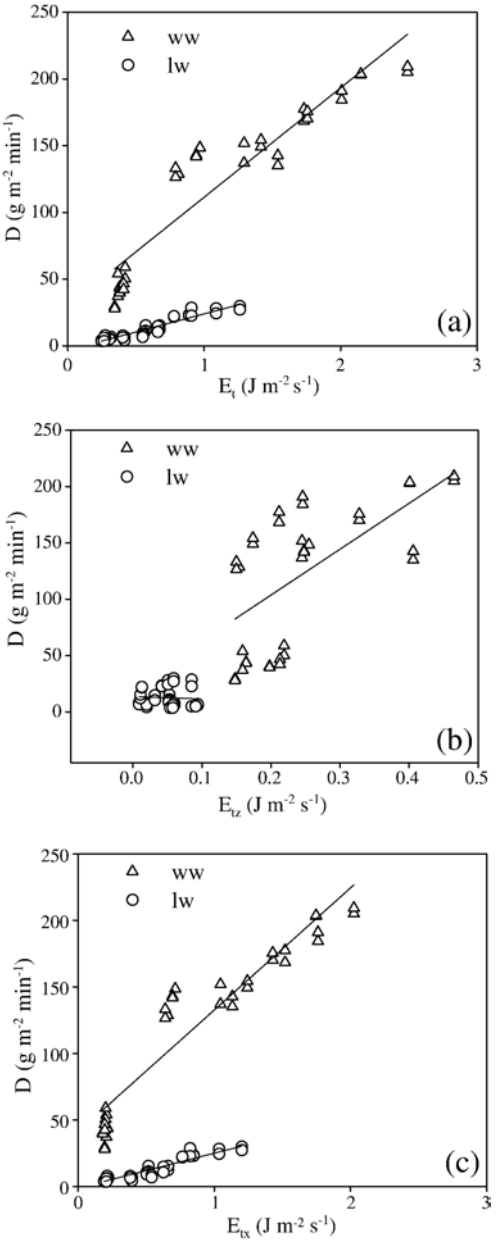

Fig. 6. Detachment rates versus Et (a), E_{tz} (b), and E_{tx} (c) differentiated for the slope aspect.

Table 4 also tabularizes the horizontal and vertical kinetic energy fluxes (E_{tx} and E_{tz}, respectively) computed by Eqs. (8) and (9). To distinguish the magnitude of each component, the ratios of the former to the latter (E_{tx}/E_{tz}) were additionally calculated (Table 4). Although the nozzle pressures make no difference in the ratios, they increased as the wind speed increased for each slope gradient and aspect. While the ratios decreased with the slope gradient in the windward slopes, they increased with it in the leeward slopes.

Also, the values clearly show that the ratios were always greater than the unity except for the rains driven by 6.4 ms^{-1} wind speed incident on the windward slopes of 9° (E_{tx}/

$E_{tz} \approx 0.98$) for all nozzle pressures, implying that in the study E_{tx} was mostly higher than E_{tz}. In particular, the ratios were as high as 60 for the rains of 12.0 ms^{-1} wind speed incident on the leeward slopes of 9° and finally there were extremely large differences in the ratio between the aspects (Table 4). As opposed to the cases under which most of the controlled studies which consider only E_{tz} in the soil and sand detachment process, were conducted, this study was performed under the cases where E_{tx} appeared to have more control over the sand detachment than E_{tz} in magnitude.

Variation of the measured sand detachment rates (D, g m^{-2} min^{-1}) (Table 4) with E_t, E_{tz}, and E_{tx} is shown in Fig. 6. In these scatter plots of sand detachment rates versus E_t, E_{tz}, and E_{tx}, data were discriminated between the slope aspects. For both windward and leeward slopes the data clustered around the line adequately in Fig. 6a, suggesting that as E_t increased, D increased. The line was steeper in the windward slopes than in the leeward slopes, suggesting that a unit increase in E_t caused more sand detachment per unit area per unit time in the windward slopes than in the leeward slopes.

Scatter plots of sand detachment rates versus E_{tz}, and E_{tx} were given in Fig. 6b and c, respectively. The data clustered around the line more tightly in Fig. 6c than in Fig. 6b. Especially, it can be seen in Fig. 6b that in the leeward slopes the E_{tz} range was so narrow that the data points could not allow a line to fit to some extent that a clear pattern could emerge. This analysis of parting data in terms of the slope aspect also indicated that different detachment rates occurred with different relative contribution of the compressive and shear stresses. When the magnitude of E_{tz} and E_{tx} was more comparable, there was more sand detachment. These cases coincided with the windward slopes. However in the leeward slopes, as decreases in E_{tz} were serious, less sand detachment took place although E_{tx} was of much greater significance. Extreme increases in E_{tx} at the expense of E_{tz} did not bring about significant increases in D.

Statistical analyses for the relationship between D (g m^{-2} s^{-1}) and E_t (J m^{-2} s^{-1}) and D and both E_{tz} and E_{tx} by the log-linear regression models are presented in Table 5. The model that accounted for the distinct effect of E_{tz} and E_{tx} on D resulted in much better coefficient of determination ($R^2 = 0.82$) than that of E_t ($R^2 = 0.63$) because E_t could not differentiate the relative role of compressive stress and shear stress in the process. For example, Fig. 6a shows that the sand detachment rates of the windward slopes significantly differed from those of the leeward slopes at the same E_t values; the variation of D with E_t in the former was

Table 5
Statistical analysis for the relationship between the sand detachment rate (D, g m^{-2} min^{-1}) and the resultant energy flux (E_t, J m^{-2} s^{-1}) and both fluxes of energy related to normal and horizontal components of the resultant velocity (E_{tz} and E_{tx}, respectively) by the log-linear regression

Model	k	a	b	R^2
$D=kE_t^a$	58.86	1.59	–	0.63
$D=kE_{tz}^a E_{tx}^b$	391.07	0.83	0.87	0.82

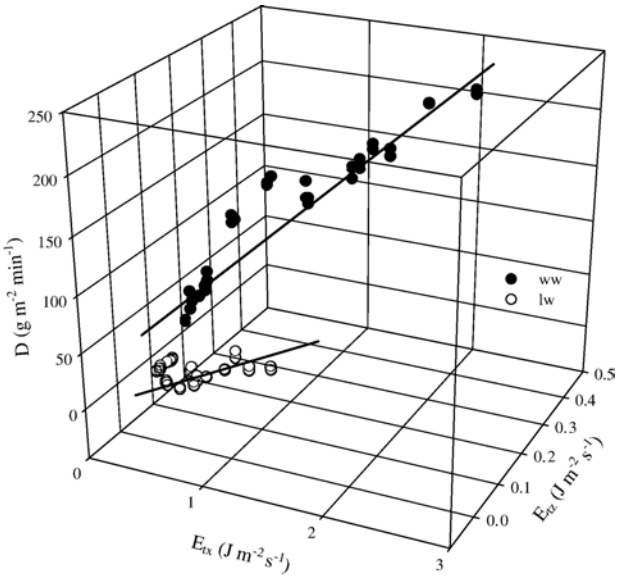

Fig. 7. Detachment rates as function of both E_{tz} and E_{tx} differentiated for the slope aspect.

greater than that of the latter since the magnitude of E_{tz} in the windward slopes was larger when compared with that of leeward slopes (Table 4). Detachment rates as function of both E_{tz} and E_{tx} differentiated for the slope aspect is shown in Fig. 7. And, a scatter plot of measured (D_m, g m^{-2} min^{-1}) versus predicted sand detachment rates (D_p, g m^{-2} min^{-1}) with the model of $D=kE_{tz}^a E_{tx}^b$ is given in Fig. 8.

Table 6 presents the Pearson correlation coefficients between D and E_t, E_{tz}, and E_{tx}. The results show that E_{tz} had a better correlation coefficient with D (0.76) than E_{tx} (0.64), implying that E_{tz} and E_{tx} accounted for 76% and 64% of the variation in D, respectively. The coefficient of E_t with D was 0.79, almost

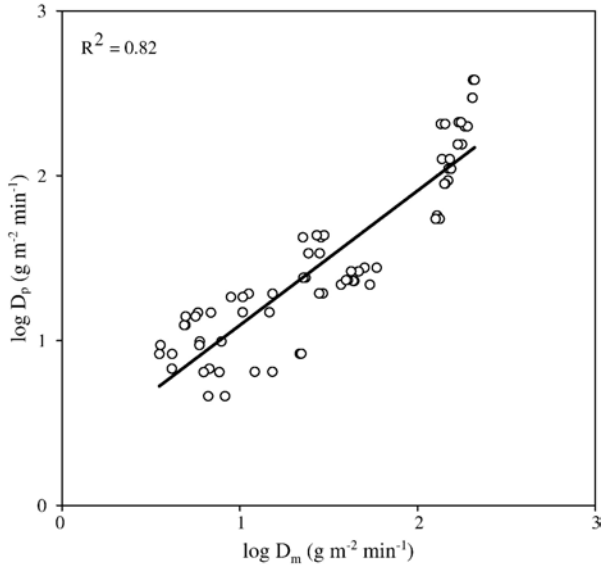

Fig. 8. Scatter plot of measured (D_m) versus predicted (D_p) sand detachment rates by a log-linear regression.

Please cite this article as: Erpul, G. et al. Sand detachment under rains with varying angle of incidence. Catena (2007), doi:10.1016/j.catena.2007.07.008

Table 6
Pearson correlation coefficients between the sand detachment rate (D, g m^{-2} min^{-1}) and the total resultant energy flux (E_t, J m^{-2} s^{-1}) and both fluxes of energy related to normal and horizontal components (E_{tz} and E_{tx}, respectively)

	E_t	E_{tz}	E_{tx}	D
E_t	1.00 (0.0000)	0.42 (0.0003)	0.97 (0.0001)	0.79 (0.0001)
E_{tz}		1.00 (0.0000)	0.21 (0.0706)	0.76 (0.0001)
E_{tx}			1	0.64 (0.0001)
D				1.00 (0.0000)

the same as that E_{tz}. This suggested that, regardless of E_{tx}, E_{tz} was as good as E_t in the sand detachment process under wind-driven rains.

4. Conclusions

Sand detachment experiments were conducted under improved lateral jetting of raindrops induced by wind velocities of 6.4, 10.0, and 12.0 m s^{-1} at nozzle operating pressures of 75, 100, and 150 kPa and incident on windward and leeward slopes of 4 and 9°. This allowed to study the effect of varying angle of incidence and to determine the partition of the compressive stress and shear stress evaluated by the horizontal and vertical kinetic energy fluxes (E_{tx} and E_{tz}, respectively) in the course of raindrop detaching action on the cohesionless sand surface. The graphical and statistical analyses indicated that in the windward slopes where the importance of E_{tz} and E_{tx} was more comparable, there was more sand detachment while in the leeward slopes where extreme increases in E_{tx} as E_{tz} particularly decreased occurred, less sand detachment resulted. A power model considering the discriminating effect of the compressive and shear stresses on the detachment produced similar exponent values to which E_{tz} and E_{tx} were raised (0.83 and 0.87, respectively); E_{tx} was as good as at the process E_{tz} in contradiction to the fact that erosion damage varies only with the normal component of impact velocity. In spite of this, the magnitude of compressive stress at last controlled the process since the sand detachment rates increased and decreased, respectively as the relative contribution of E_{tz} increased and decreased although E_{tx} attained at very high values.

References

Al-Durrah, M.M., Bradford, J.M., 1982. The mechanism of raindrop splash on soil surfaces. Soil Science Society of America Journal 46, 1086–1090.

Blocken, B., Carmeliet, J., 2000. Driving rain on building envelopes — I: numerical estimation and full-scale experimental verification. Journal of Thermal Envelope & Building Science 24 (1), 61–85.

Blocken, B., Carmeliet, J., 2002. Spatial and temporal distribution of driving rain on a low-rise building. Wind and Structures 5 (5), 441–462.

Blocken, B., Carmeliet, J., 2004. A review of wind-driven rain research in building science. Journal of Wind Engineering and Industrial Aerodynamics 92 (13), 1079–1130.

Blocken, B., Carmeliet, J., Poesen, J., 2005. Numerical simulation of the wind-driven rain distribution over smallscale topography in space and time. Journal of Hydrology 315, 252–273.

Blocken, B., Poesen, J., Carmeliet, J., 2006. Impact of wind on the spatial distribution of rain over micro-scale topography — numerical modelling and experimental verification. Hydrological Processes 20 (2), 345–368.

Cornelis, W., Erpul, G., Gabriels, D., 2004a. The I.C.E. wind tunnel for wind and water interaction research. Wind and rain interaction in erosion. In: Visser, S., Cornelis, W. (Eds.), Tropical Resource Management Papers, Chapter 13. Wageningen University and Research Centre, pp. 195–224.

Cornelis, W.M., Oltenfreiter, G., Gabriels, D., Hartmann, R., 2004b. Splash-saltation of sand due to wind-driven rain: vertical deposition flux and sediment transport rate. Soil Science Society of America Journal 68, 32–40.

Cornelis, W.M., Oltenfreiter, G., Gabriels, D., Hartmann, R., 2004c. Splash-saltation of sand due to wind-driven rain: horizontal flux and sediment transport rate. Soil Science Society of America Journal 68, 41–46.

Cruse, R.M., Berghoefer, B.E., Mize, C.W., Ghaffarzadeh, M., 2000. Water drop impact angle and soybean protein amendment effects on soil detachment. Soil Science Society of America Journal 64, 1474–1478.

De Lima, J.L.M.P., 1989. Raindrop splash anisotropy: slope, wind, and overland flow velocity effects. Soil Technology 2, 71–78.

De Lima, J.L.M.P., 1990. The effect of oblique rain on inclined surfaces: a nomograph for the rain-gauge correction factor. Journal of Hydrology 115, 407–412.

Ellison, W.D., 1947. (7 parts). Soil erosion studies. Agricultural Engineering 28, 145–146; 197–201; 245–248; 297–300; 349–351; 407–408; 447–450.

Erpul, G., 1996. Determination of rainfall characteristics in a wind tunnel. M.Sc. Thesis, Ghent University, Ghent. 106 pp.

Erpul, G., 2001. Detachment and sediment transport from interrill areas under wind-driven rains. Ph.D. thesis. Purdue University, West Lafayette, IN.

Erpul, G., Gabriels, D., Janssens, D., 1998. Assessing the drop size distribution of simulated rainfall in a wind tunnel. Soil and Tillage Research 45, 455–463.

Erpul, G., Gabriels, D., Janssens, D., 2000. The effect of wind on size and energy of small simulated raindrops: a wind tunnel study. International Agrophysics 14, 1–7.

Erpul, G., Norton, L.D., Gabriels, D., 2003. The effect of wind on raindrop impact and rainsplash detachment. Transactions of the American Society of Agricultural Engineering 45 (6), 51–62.

Erpul, G., Norton, L.D., Gabriels, D., 2004. Splash-saltation trajectories of soil particles under wind-driven rain. Geomorphology 59, 31–42.

Erpul, G., Gabriels, D., Norton, L.D., 2005. Sand detachment by wind-driven raindrops. Earth Surface Processes and Landforms 30, 241–250.

Furbish, D.J., Hamner, K.K., Schmeeckle, M., Borosund, M.N., Mudd, S.M., 2007. Rain splash of dry sand revealed by high-speed imaging and sticky paper splash targets. Journal of Geophysical Research—Earth Surface 112 (F1) (Art. No. F01001).

Gabriels, D., Cornelis, W., Pollet, I., Van Coillie, T., Quessar, M., 1997. The I. C. E. wind tunnel for wind and water erosion studies. Soil Technology 10, 1–8.

Ghadiri, H., 2004. Crater formation in soils by raindrop impact. Earth Surface Processes and Landforms 29, 77–89.

Ghadiri, H., Payne, D., 1981. Raindrop impact stress. Journal of Soil Science 32, 41–49.

Ghadiri, H., Payne, D., 1986. The risk of leaving soil surface unprotected against falling rain. Journal of Soil and Tillage Research 8, 119–130.

Ghadiri, H., Payne, D., 1988. The formation and characteristics of splash following raindrop impact on soil. Journal of Soil Science 39, 563–575.

Hairsine, P.B., Rose, C.W., 1991. Rainfall detachment and deposition: sediment transport in the absence of flow driven processes. Soil Science Society of America Journal 55, 320–324.

Huang, C., Bradford, J.M., Cushman, J.H., 1982. A numerical study of raindrop impact phenomena: the rigid case. Soil Science Society of America Journal 46, 14–19.

Huang, C., Bradford, J.M., Cushman, J.H., 1983. A numerical study of raindrop impact phenomena: the elastic deformation case. Soil Science Society of America Journal 47, 855–866.

Kinnell, P.I.A., 1981. Rainfall intensity — kinetic energy relationship for soil loss prediction. Soil Science Society of America Journal 45, 153–155.

Meyer, L.D., 1981. How rain intensity affects interrill erosion. Transactions of the American Society of Agricultural Engineering 24, 1472–1475.

Morgan, R.P.C., 1978. Field studies of rainsplash erosion. Earth Surface Processes 3, 295–299.

Park, S.W., Mitchell, J.K., Bubenzer, G.D., 1983. Rainfall characteristics and their relation to splash erosion. Transactions of the American Society of Agricultural Engineering 26, 795–804.

Please cite this article as: Erpul, G. et al. Sand detachment under rains with varying angle of incidence. Catena (2007), doi:10.1016/j.catena.2007.07.008

Poesen, J., 1985. An improved splash transport model. Zeitschrift fur Geomorphologie N.F. 29, 193–221.

Poesen, J., Savat, J., 1981. Detachment and transportation of loose sediments by raindrop splash. Part II: detachability and transportability measurements. Catena 8, 19–41.

Poesen, J., Torri, D., 1988. The effect of cup size on splash detachment and transport measurements. Part I: field measurements. Catena. Supplement 12, 113–126.

Salles, C., Poesen, J., 2000. Rain properties controlling soil splash detachment. Hydrological Processes 14, 271–282.

Savat, J., Poesen, J., 1981. Detachment and transportation of loose sediments by raindrop splash. Part I: the calculation of absolute data on detachability and transportability. Catena 8, 1–18.

Sensit, 2000. Model V04 kinetic energy of rain sensor software. Sensit Company, Portland, N.D.

Sharma, P.P., Gupta, S.C., 1989. Sand detachment by single raindrops of varying kinetic energy and momentum. Soil Science Society of America Journal 53, 1005–1010.

Sharma, P.P., Gupta, S.C., Rawls, W.J., 1991. Soil detachment by single raindrops of varying kinetic energy. Soil Science Society of America Journal 55, 301–307.

Sharma, P.P., Gupta, S.C., Foster, G.R., 1995. Raindrop-induced soil detachment and sediment transport from interrill areas. Soil Science Society of America Journal 59, 727–734.

Sharon, D., 1970. Topography-conditioned variations in rainfall as related to the runoff contributing areas in a small watershed. Israel Journal of Earth-Sciences 19, 85–89.

Sharon, D., 1980. The distribution of hydrologically effective rainfall incident on sloping ground. Journal of Hydrology 46, 165–188.

Sharon, D., Arazi, A., 1997. The distribution of wind-driven rain in a small valley: an empirical basis for numerical model verification. Journal of Hydrology 201, 21–48.

Sharon, D., Adar, E., Lieberman, G., 1983. Observations on the differential hydrological and/or erosional response of opposite-lying slopes, as related to incident rainfall. Israel Journal of Earth-Sciences 32, 71–74.

Sharon, D., Morin, J., Moshe, Y., 1988. Micro-topographical variations of rainfall incident on ridges of a cultivated field. Transactions of the ASAE 31 (6), 1715–1722.

Springer, G.S., 1976. Erosion by liquid impact. John Wiley and Sons, Inc., New York.

Van Heerden, W.M., 1964. Splash erosion as affected by the angle of incidence of raindrop impact. Unpublished Ph.D. thesis. Purdue University, Lafayette, Ind. USA.

Young, R.A., Wiersma, J.L., 1973. The role of rainfall impact in soil detachment and transport. Water Resources Research 9 (6), 1629–1636.

Please cite this article as: Erpul, G. et al. Sand detachment under rains with varying angle of incidence. Catena (2007), doi:10.1016/j.catena.2007.07.008